Cell Reports
Article

Suppression of Nucleotide Metabolism Underlies the Establishment and Maintenance of Oncogene-Induced Senescence

Katherine M. Aird,[1] Gao Zhang,[2] Hua Li,[1] Zhigang Tu,[1] Benjamin G. Bitler,[1] Azat Garipov,[1] Hong Wu,[3] Zhi Wei,[4] Stephan N. Wagner,[5,6] Meenhard Herlyn,[2] and Rugang Zhang[1,*]
[1]Gene Expression and Regulation Program
[2]Tumor Microenvironment and Metastasis Program
The Wistar Institute Cancer Center, The Wistar Institute, Philadelphia, PA 19104, USA
[3]Department of Pathology, Fox Chase Cancer Center, Philadelphia, PA 19111, USA
[4]Department of Computer Science, New Jersey Institute of Technology, Newark, NJ 07102, USA
[5]Division of Immunology, Allergy and Infectious Diseases, Department of Dermatology, Medical University of Vienna, Waehringer Guertel 18-20, 1090 Vienna, Austria
[6]CeMM Research Center for Molecular Medicine of the Austrian Academy of Sciences, Lazarettgasse 14, 1090 Vienna, Austria
*Correspondence: rzhang@wistar.org
http://dx.doi.org/10.1016/j.celrep.2013.03.004

SUMMARY

Oncogene-induced senescence is characterized by a stable cell growth arrest, thus providing a tumor suppression mechanism. However, the underlying mechanisms for this phenomenon remain unknown. Here, we show that a decrease in deoxyribonucleotide triphosphate (dNTP) levels underlies oncogene-induced stable senescence-associated cell growth arrest. The decrease in dNTP levels is caused by oncogene-induced repression of ribonucleotide reductase subunit M2 (RRM2), a rate-limiting protein in dNTP synthesis. This precedes the senescence-associated cell-cycle exit and coincides with the DNA damage response. Consistently, RRM2 down-regulation is both necessary and sufficient for senescence. Strikingly, suppression of nucleotide metabolism by RRM2 repression is also necessary for maintenance of the stable senescence-associated cell growth arrest. Furthermore, RRM2 repression correlates with senescence status in benign nevi and melanoma, and its knockdown drives senescence of melanoma cells. These data reveal the molecular basis whereby the stable growth arrest of oncogene-induced senescence is established and maintained through suppression of nucleotide metabolism.

INTRODUCTION

Cellular senescence is defined as a state of stable cell growth arrest (Campisi, 2005). Activation of oncogenes, such as RAS, in normal mammalian cells typically triggers oncogene-induced senescence (OIS) (Yaswen and Campisi, 2007), which is a bona fide tumor suppressor mechanism in vivo (Campisi and d'Adda di Fagagna, 2007). For example, benign nevi formed by human melanocytes that have undergone OIS are thought to suppress melanomagenesis (Mooi and Peeper, 2006). Although known to be important for tumor suppression, to date, the molecular mechanism underlying the stable OIS-associated cell growth arrest remains unknown.

Oncogenic signaling triggers cellular senescence via various senescence effectors. In particular, senescence induced by activated oncogenes such as RAS is characterized by a sustained DNA damage response (DDR) triggered by aberrant DNA replication during the S phase of the cell cycle (Bartkova et al., 2006; Di Micco et al., 2006). This ultimately activates the p53/p21 and p16/pRB pathways (Serrano et al., 1997). Activation of these signaling pathways cultivates the expression of markers of senescence such as senescence-associated heterochromatin foci (SAHF), which are specialized domains of facultative heterochromatin that contribute to senescence by silencing proliferation-promoting genes (Narita et al., 2003; Zhang et al., 2007a), and increased senescence-associated β-galactosidase (SA-β-gal) activity (Dimri et al., 1995).

Cellular deoxyribonucleotide triphosphate (dNTP) levels play a key role in regulating DNA replication and, consequently, cell proliferation (Reichard, 1988). However, whether changes in the nucleotide metabolic pathway play a role in regulating OIS-associated stable cell growth arrest has never been investigated. Ribonucleotide reductase (RNR) plays a key role in dNTP biogenesis (Nordlund and Reichard, 2006). RNR is a tetrameric complex consisting of two large catalytic subunits (termed RRM1) and two small regulatory subunits (RRM2 or p53R2) (Nordlund and Reichard, 2006). Notably, RRM2 is the regulatory subunit that controls dNTP synthesis during the S phase of the cell cycle, whereas RRM1 is present throughout the cell cycle (Engström et al., 1985). Importantly, RRM2 expression is rate-limiting for RNR activity (Nordlund and Reichard, 2006). In contrast, p53R2 is involved in supplying dNTPs for DNA repair and mitochondrial DNA synthesis in the G0/G1 phase of the cell cycle (Håkansson et al., 2006). Whether RRM2 plays a role in

regulating OIS, which is characterized by aberrant DNA replication, the DDR, and a stable cell growth arrest, has never been investigated.

Here, we report that a decrease in dNTP levels underlies the establishment and maintenance of the stable OIS-associated cell growth arrest. We show that addition of exogenous nucleosides is sufficient to overcome OIS-associated cell growth arrest, which correlates with suppressing aberrant DNA replication and inhibiting the DDR. Mechanistically, we discovered that the decrease in dNTP levels is caused by oncogene-induced suppression of RRM2 expression. This correlates with the recruitment of E2F7, an atypical E2F transcriptional repressor, to its promoter. Indeed, we show that RRM2 downregulation is both necessary and sufficient for the establishment and maintenance of the stable senescence-associated cell growth arrest. Further underscoring the importance of this pathway in regulating senescence in human cancers, we show that RRM2 expression inversely correlates with senescence status in human nevi and melanoma specimens harboring oncogenic BRAF or NRAS. Additionally, high RRM2 expression correlates with poor overall survival in patients with melanoma with oncogenic BRAF or NRAS. Finally, knockdown of RRM2 drives senescence of melanoma cells harboring these activated oncogenes. Taken together, our results reveal the mechanistic basis whereby an activated oncogene establishes and maintains the stable senescence-associated cell growth arrest by suppressing nucleotide metabolism.

RESULTS

Exogenous Nucleosides Suppress OIS and Its Associated Cell Growth Arrest

Senescent cells are characterized by a stable cell growth arrest (Campisi, 2005), and nucleotide metabolism plays a critical role in regulating cell growth (Reichard, 1988). To test the hypothesis that nucleotide metabolism regulates OIS, IMR90 primary human fibroblasts were infected with RAS-encoding retrovirus to induce senescence (Figure S1A), and exogenous nucleosides were added at the time of infection. Compared with controls, addition of exogenous nucleosides significantly suppressed the expression of markers of senescence such as SAHF formation (Figures 1A and 1B), SA-β-gal activity (Figures 1A and 1B), and the upregulation of p16, p21, and p53 (Figure 1C). In addition, senescence induced by oncogenic RAS is characterized by the DDR (Bartkova et al., 2006; Di Micco et al., 2006). Thus, we examined markers of the DDR such as formation of γH2AX foci in these cells. Compared with controls, addition of exogenous nucleosides significantly decreased γH2AX foci formation (Figures 1D and 1E). Next, we determined the effects of exogenous nucleosides on the senescence-associated cell-cycle exit by bromodeoxyuridine (BrdU) incorporation. Exogenous nucleosides significantly increased BrdU incorporation in RAS-infected cells compared with controls (Figures 1F and 1G). Finally, we sought to determine the effects of exogenous nucleosides on the OIS-associated cell growth arrest by colony-formation and cell growth curve assays. Compared with RAS-alone controls, there was a significant increase in colony formation (Figure 1H) and cell growth (Figure 1I) in exogenous nucleoside-supplemented cells. Interestingly, senescence induced by DNA damage reagents such as doxorubicin or etoposide was not affected by addition of exogenous nucleosides (Figures S1B–S1I), suggesting that the observed effects are not merely a consequence of DNA damage. Based on these results, we conclude that exogenous nucleosides added at the time of infection are sufficient to suppress OIS and its associated cell growth arrest.

Exogenous Nucleosides Are Sufficient to Overcome the OIS-Associated Cell Growth Arrest in Established Senescent Cells

We next wanted to determine the effects of exogenous nucleosides on the stable OIS-associated cell growth arrest in established senescent cells. To do so, stable senescence-associated cell growth arrest was established by culturing RAS-infected cells for 6 days, as evidenced by the minimal BrdU incorporation in these cells compared with controls as well as no appreciable cell growth during the experimental period (Figures S2A–S2C). Then FACS was performed with C_{12}FDG, a fluorogenic substrate for SA-β-gal activity in live cells (Debacq-Chainiaux et al., 2009) (Figure 2A). FACS-sorted senescent cells were further cultured with or without exogenous nucleosides. We then examined the expression of markers of senescence and proliferation in these cells. Compared with controls, markers of senescence such as SA-β-gal activity and p16 and p21 expression were all suppressed by exogenous nucleosides (Figures 2B–2D). In contrast, markers of cell proliferation, such as BrdU incorporation, were increased in the established senescent cells exposed to exogenous nucleosides (Figure 2E). Strikingly, addition of exogenous nucleosides to these cells reversed the oncogene-induced stable senescence-associated cell growth arrest, as evidenced by marked growth of these cells (Figure 2F). Notably, these observations were not due to a loss of RAS expression because RAS was expressed at similar levels in these cells compared to those without exposure to exogenous nucleosides (Figure S2D). Similar observations were also made when RAS cells were allowed to senescence for a longer period of time (e.g., exogenous nucleosides added at day 12; Figures S2E–S2G). Likewise, we also observed similar effects of exogenous nucleosides in another primary human fibroblast cell line, WI38 (Figures S2H–S2J), demonstrating that this is not a cell line-specific phenomenon. Interestingly, withdrawal of nucleosides from these cells was sufficient for the cells to senesce again, as shown by an increase in SA-β-gal activity (Figures 2G and 2H) and p21 and p16 expression (Figure 2I), and a decrease in both cyclin A expression (Figure 2I) and cell growth (Figure 2J). Taken together, these data indicate that addition of exogenous nucleosides is sufficient to overcome the stable OIS-associated cell growth arrest in established senescent cells.

A Decrease in dNTP Levels Occurs Prior to the OIS-Associated Cell-Cycle Exit

Because addition of exogenous nucleosides suppresses senescence (Figures 1 and 2), we next sought to determine whether changes in dNTP levels occur during OIS. Toward this goal, we measured dNTP levels in control and RAS-infected IMR90 cells. To limit the potential effects of cell cycle and cell proliferation status on dNTP levels, we performed a detailed time course

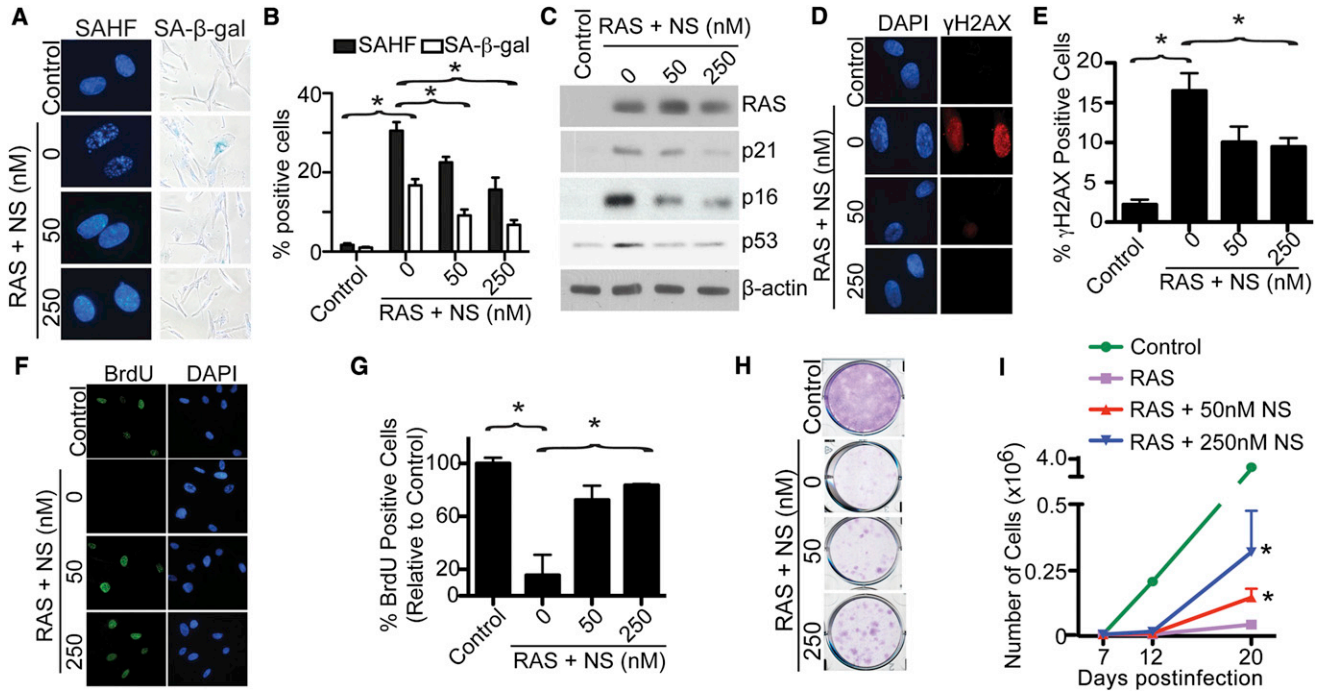

Figure 1. Exogenous Nucleosides Suppress OIS and Its Associated Cell Growth Arrest

(A) IMR90 cells were infected with control or RAS-encoding retrovirus with or without addition of the indicated concentration of nucleosides (NS) at the time of infection. On day 6, drug-selected cells were examined for SAHF formation and SA-β-gal activity.

(B) Quantification of (A). Mean of three independent experiments with SEM is shown. *$p < 0.05$.

(C) Same as (A) but examined for expression of RAS, p21, p16, p53, and β-actin by immunoblotting.

(D) Same as (A) but stained for γH2AX foci formation. DAPI counterstaining was used to visualize nuclei.

(E) Quantification of (D). Mean of three independent experiments with SEM is shown. *$p < 0.05$.

(F) Same as (A) but labeled with BrdU for 1 hr. The incorporated BrdU was visualized by immunofluorescence. DAPI counterstaining was used to visualize nuclei.

(G) Quantification of (F). Mean of three independent experiments with SEM is shown. *$p < 0.01$.

(H) Same as (A), but an equal number of cells were inoculated in 6-well plates. After 2 weeks, the plates were stained with 0.05% crystal violet in PBS to visualize colony formation. Shown are representative images of three independent experiments.

(I) Same as (A), but an equal number of cells were seeded in 6-well plates. The number of cells was counted at the indicated time points after infection. Mean of three independent experiments with SEM is shown. *$p < 0.05$ compared with RAS-alone cells.

See also Figure S1.

analysis for cell-cycle distribution using FACS analysis, markers of cell proliferation such as serine 10 phosphorylated histone H3 (pS10H3), and markers of senescence such as p21 and p16 (Figures S3A and S3B). Based on the time course analysis, we determined the dNTP levels on day 2, which is prior to the cell-cycle exit, as further demonstrated by comparable BrdU incorporation and cyclin A expression in RAS-infected cells compared to controls (Figures S3C–S3E). Strikingly, the levels of all four dNTPs were significantly decreased in RAS-infected cells compared with controls at this time point (Figure 3A). Together, these data support the idea that there is a decrease in dNTP levels, which occurs prior to the OIS-associated cell-cycle exit.

Addition of exogenous nucleosides suppresses OIS-associated DDR (Figures 1C–1E), which is triggered by aberrant DNA replication (Bartkova et al., 2006; Di Micco et al., 2006). Moreover, RAS significantly decreases dNTP levels prior to the senescence-associated cell-cycle exit (Figure 3A). Thus, we sought to determine whether the decrease in dNTP levels plays a role in regulating aberrant DNA replication induced by oncogenic RAS. Toward this goal, we determined the changes in the dynamics of DNA replication in control and RAS-infected cells with or without exogenous nucleosides using the DNA-combing analysis (Figures S3F and S3G). This allows for observation of single-stranded DNA (ssDNA) to determine DNA replication fork dynamics (namely elongating, terminated, and newly fired, as illustrated in Figure S3G). Indeed, addition of exogenous nucleosides significantly rescued the aberrant DNA replication observed during RAS-induced senescence (Figure 3B). Notably, this correlates with a significant restoration of dNTP levels in RAS-infected cells supplemented with exogenous nucleosides (Figure 3C). This result is consistent with the idea that the observed effects are due to restoration of dNTP levels. Together, these results support the premise that a decrease in dNTP levels contributes to the aberrant DNA replication observed during RAS-induced senescence.

Oncogene-Induced Repression of RRM2 Occurs Prior to the Senescence-Associated Cell-Cycle Exit

We next wanted to determine the molecular mechanism whereby dNTP levels decrease during OIS. RNR is a key enzyme

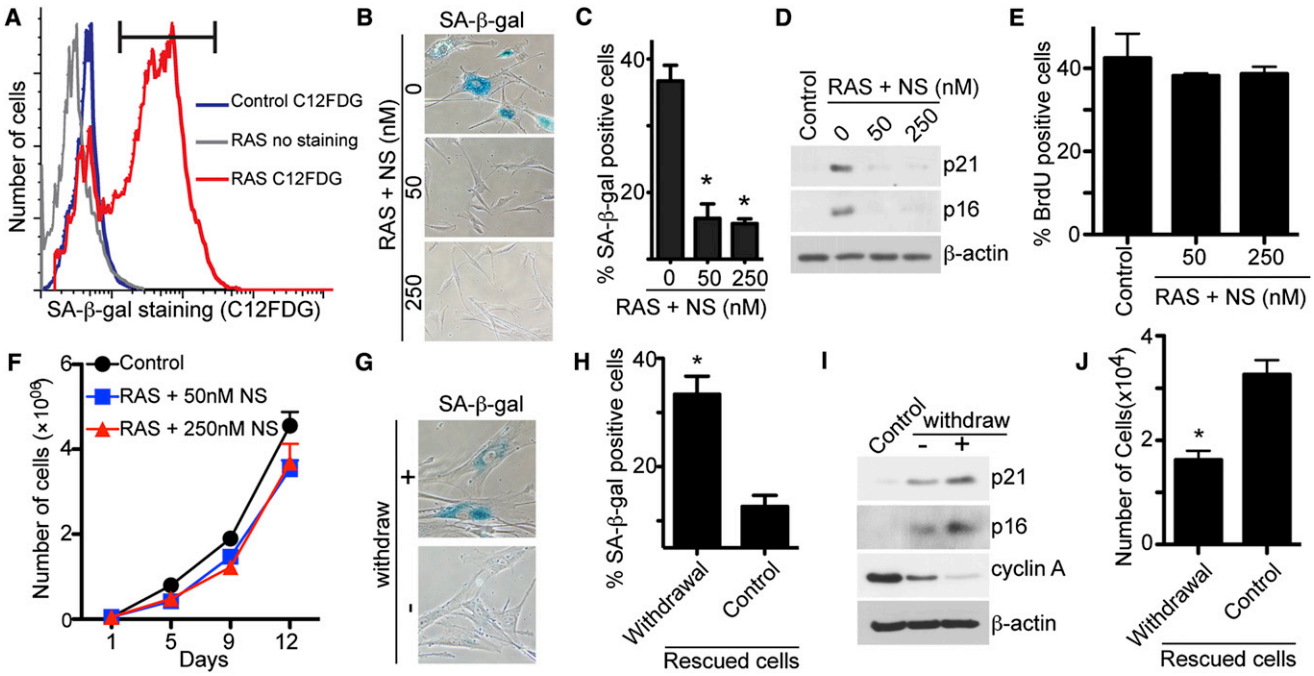

Figure 2. Exogenous Nucleosides Are Sufficient to Overcome the Stable OIS-Associated Cell Growth Arrest in Established Senescent Cells

(A) IMR90 cells were infected with RAS-encoding retrovirus. On day 6, drug-selected cells were subjected to flow cytometric sorting (FACS) of SA-β-gal-positive cells using C_{12}FDG as a substrate. Black bar indicates the gate used for sorting.

(B) FACS-sorted senescent cells were cultured without or with indicated concentrations of nucleosides for an additional 14 days. The cells were then stained for SA-β-gal activity.

(C) Quantification of (B). Mean of three independent experiments with SEM is shown. *$p < 0.001$.

(D) Same as (B) but examined for p16, p21, and β-actin expression by immunoblotting.

(E) Same as (B) but labeled with BrdU for 1 hr. Mean of three independent experiments with SEM is shown.

(F) Same as (B), but an equal number of cells that overcome senescence or control (parental) cells were inoculated in 6-well plates, and the number of cells was counted at the indicated time points. Mean of three independent experiments with SEM is shown.

(G) Cells that overcome senescence in the presence of exogenous nucleosides (50 nM) isolated from (B) (rescued cells) were continually cultured in the presence of NS (control) or withdrawn from NS exposure for an additional 17 days and stained for SA-β-gal activity.

(H) Quantification of (G). Mean of three independent experiments with SEM is shown. *$p < 0.01$.

(I) Same as (G) but examined for p21, p16, cyclin A, and β-actin expression by immunoblotting.

(J) Same as (G), but an equal number of cells were inoculated in 6-well plates after withdrawal, and the number of cells was counted 4 days later. Mean of three independent experiments with SEM is shown. *$p < 0.05$.

See also Figure S2.

in dNTP biosynthesis, and RRM2, the regulatory subunit of RNR, is rate-limiting for this process (Nordlund and Reichard, 2006). Thus, we sought to determine whether RRM2 expression is regulated during OIS. To do so, we examined the protein levels of RRM2 in control and RAS-infected cells in a detailed time course study comparing the kinetics of RRM2 expression with the expression of markers of cell proliferation such as cyclin A and pS10H3. Strikingly, as early as day 1, when RAS cells are still proliferating based on the expression of cyclin A and pS10H3 (Figures 4A and S3B), RRM2 protein expression was already decreased in RAS-infected cells compared to controls (Figure 4A). At this time point, expression of other regulators of dNTP metabolism, namely RRM1 and p53R2, was not decreased (Figure S4A), demonstrating that this is specific to RRM2. We next sought to determine the changes in RRM2 expression in cycling cells by staining for the RRM2 protein in BrdU-positive cells (transiently labeled for 1 hr). The RRM2-staining signal was specific because knockdown of RRM2 protein decreased the immunofluorescent signal (Figure S4B). Indeed, RRM2 protein expression was decreased even in BrdU-positive RAS-infected cells (Figure 4B). Notably, RRM2 downregulation coincided with the DDR as evidenced by the accumulation of γH2AX (Figure 4A), suggesting that downregulation of RRM2 may contribute to the DDR observed during OIS. However, RRM2 downregulation was not a consequence of the DDR because ionizing radiation, which induces DNA damage, failed to suppress RRM2 expression (Figure S4C). Together, these results indicate that RRM2 is downregulated prior to the OIS-associated cell-cycle exit and coincides with activation of the DDR during senescence.

We next sought to determine the molecular mechanism underlying downregulation of RRM2 during OIS. First, we asked whether RRM2 is downregulated at the transcriptional level. Accordingly, quantitative RT-PCR (qRT-PCR) was performed in

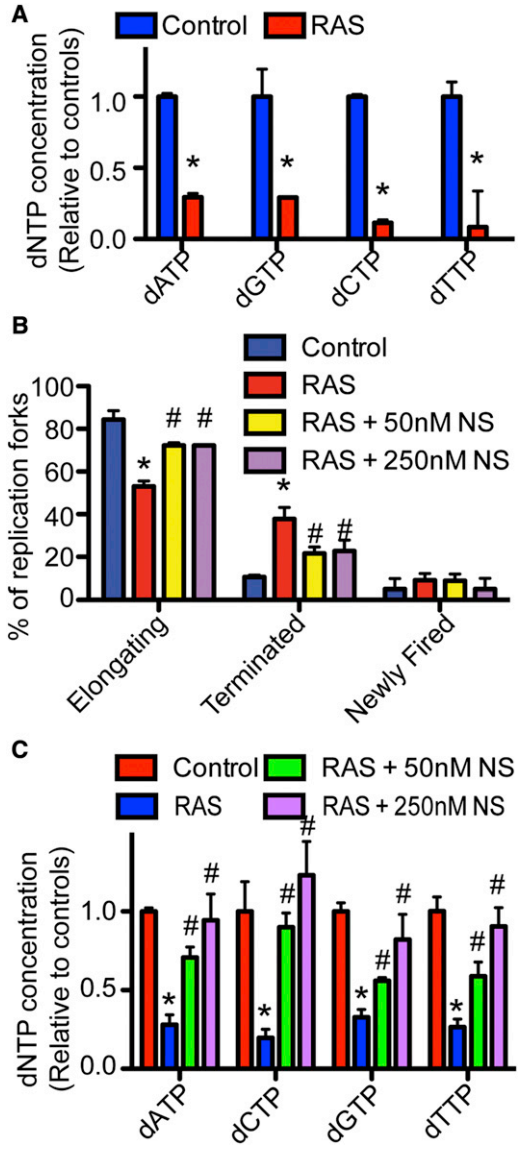

Figure 3. A Decrease in dNTP Levels Occurs Prior to the OIS-Associated Cell-Cycle Exit

(A) IMR90 cells were infected with control or RAS-encoding retrovirus. On day 2, cellular dNTP levels were measured. Mean of three independent experiments with SEM is shown. *$p < 0.05$.

(B) Same as (A), but RAS-infected cells were supplemented with or without the indicated concentration of nucleosides at the time of infection. Mean of three independent experiments with SEM is shown. *$p < 0.05$ control versus RAS; #$p < 0.05$ RAS versus RAS plus 50 or 250 nM NS.

(C) Same as (B), but cellular dNTP levels were measured. Mean of three independent experiments with SEM is shown. *$p < 0.05$ versus control; #$p < 0.05$ versus RAS alone.

See also Figure S3.

control and RAS-infected cells. Similar to RRM2 protein expression, *RRM2* mRNA expression was significantly decreased after RAS infection but prior to the senescence-associated cell-cycle exit (i.e., at day 1; Figure 4C). Consistent with the idea that decreased *RRM2* mRNA expression is due to decreased transcription, there was a significant decrease in the activity of the cloned human *RRM2* gene proximal promoter (−1,071 to +76) in the RAS-infected cells compared with controls (Figures 4D and S4D). Together, we conclude that RRM2 is downregulated at the transcriptional level, and this occurs before the senescence-associated cell-cycle exit.

To identify the transcription factor that contributes to RRM2 repression during senescence, systematic promoter mapping was performed. Notably, an E2F binding site within the proximal promoter (−998 to −991) was identified to contribute to the suppression of *RRM2* transcription in response to RAS (Figure 4D; data not shown). Deletion of the E2F binding site in the *RRM2* promoter significantly restored promoter activity in RAS-infected cells (Figure 4D). Chromatin immunoprecipitation (ChIP) experiments using an E2F1 antibody demonstrated that the binding of transcriptional activator E2F1 to the human *RRM2* gene promoter was significantly reduced in RAS-infected cells compared with controls (Figure 4E). Interestingly, RRM2 is downregulated, whereas the cells are highly proliferative, and other E2F1 target genes such as cyclin A remain highly expressed (e.g., Figure 4A). These results suggest that the RRM2 downregulation observed during OIS is context dependent. To further determine the mechanism of RRM2 downregulation, we performed ChIP analysis using antibodies to the repressive E2F transcriptional factors E2F4 and E2F7 (Chen et al., 2009). These data demonstrate that binding of the atypical transcriptional repressor E2F7 to the human *RRM2* gene promoter was significantly enhanced in RAS-infected cells compared to controls (Figure 4E), whereas there was no change in E2F4 binding (data not shown). Indeed, a detailed time course study revealed that downregulation of RRM2 coincides with upregulation of E2F7 during RAS-induced senescence (Figure 4F). These results indicate that an enhanced association of the atypical transcriptional repressor E2F7 with the *RRM2* gene promoter and a simultaneous decrease in binding of transcriptional activator E2F1 to the *RRM2* gene promoter contribute to downregulation of RRM2 prior to the OIS-associated cell-cycle exit.

Knockdown of RRM2 Induces Senescence in Primary Human Fibroblasts

We next wanted to determine whether RRM2 downregulation is sufficient to induce senescence. To do so, we infected cells with lentivirus encoding small hairpin RNAs to the human *RRM2* gene (shRRM2). The knockdown efficacy of shRRM2 was confirmed by qRT-PCR and immunoblotting (Figures 5A and S5A). Consistent with the hypothesis that RRM2 downregulation decreases the dNTP levels observed during senescence, we determined that knockdown of RRM2 caused a significant decrease in dNTP levels (Figure S5B). In addition, we determined that knockdown of RRM2 triggers aberrant DNA replication (Figures 5B and S5C). Furthermore, DDR markers such as formation of 53BP1 and γH2AX foci were significantly induced by shRRM2 (Figures 5C, 5D, S5D, and S5E). Likewise, γH2AX and p53 protein expression was upregulated in shRRM2-expressing cells compared to controls (Figures 5E and S5F). Together, these results support the idea that a decrease in dNTP levels caused by RRM2 downregulation drives aberrant DNA replication and consequently the DDR observed during OIS.

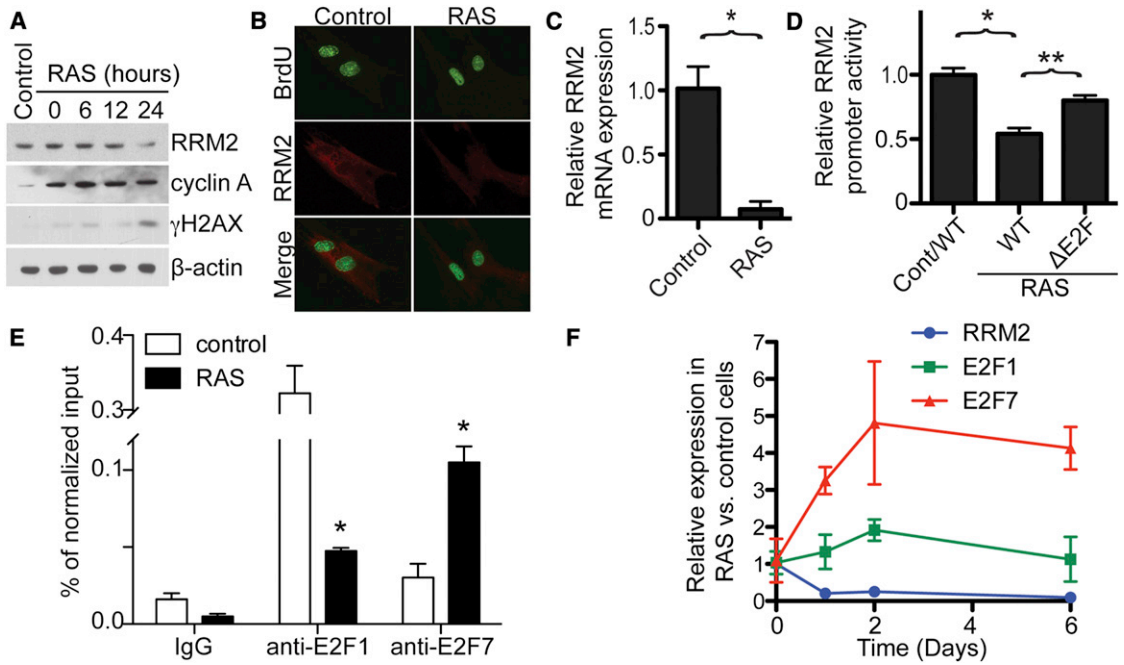

Figure 4. Oncogene-Induced Repression of RRM2 Occurs Prior to the OIS-Associated Cell-Cycle Exit

(A) IMR90 cells were infected with control or RAS-encoding retrovirus. The expression of RRM2, cyclin A, γH2AX, and β-actin was determined by immunoblotting at the indicated time points after completing RAS infection.

(B) IMR90 cells were infected with control or RAS-encoding retrovirus. On day 1, the infected cells were labeled with BrdU for 1 hr, and the expression of RRM2 in BrdU-incorporated cells was visualized by immunofluorescence.

(C) Same as (A), but cells were examined for RRM2 mRNA expression by qRT-PCR on day 1. Mean of three independent experiments with SEM is shown. *$p < 0.01$.

(D) On day 2, drug-selected control or RAS-infected cells were electroporated with a luciferase reporter driven by a WT or E2F binding site-deleted (ΔE2F) mutant human proximal *RRM2* gene promoter. A luminescent β-gal reporter was used as an internal control to normalize the transfection efficacy. Mean of three independent experiments with SEM is shown. *$p < 0.001$ Control/WT versus RAS/WT; **$p < 0.05$ WT versus ΔE2F.

(E) Same as (C), but cells were examined for E2F1 and E2F7 binding to the *RRM2* promoter by ChIP using an E2F1 or E2F7 antibody. An isotype-matched IgG was used as a control. Mean of three independent experiments with SEM is shown. *$p < 0.001$.

(F) IMR90 cells were infected with control or RAS-encoding retrovirus. Expression of RRM2, E2F1, and E2F7 mRNA was determined by qRT-PCR at the indicated time points. Mean of three independent experiments with SEM is shown.

See also Figure S4.

We next determined whether knockdown of RRM2 is sufficient to induce senescence and the associated cell-cycle exit. Compared with controls, markers of senescence such as SA-β-gal activity (Figures 5F, 5G, S5G, and S5H) were induced by RRM2 knockdown. Consistently, markers of cell proliferation, including expression of cyclin A and pS10H3 (Figures 5H and S5I) and BrdU incorporation (Figures 5I, 5J, S5J, and S5K), were lower in shRRM2-expressing cells. Indeed, senescence-associated cell growth arrest was evident in RRM2 knockdown cells, as demonstrated by assays such as colony formation (Figures 5K and S5L) and cell growth curves (Figure 5L). Together, we conclude that knockdown of RRM2 induces cellular senescence in primary human fibroblasts.

To limit the potential off-target effects of shRNAs, we performed rescue experiments by infecting cells with a retrovirus encoding a wild-type (WT) RRM2 cDNA together with a lentivirus encoding an shRRM2 that targets the 5′ UTR of the human *RRM2* gene. Knockdown of endogenous RRM2 was confirmed by downregulation of RRM2 mRNA measured by qRT-PCR using primers targeting the 5′ UTR (Figure 5A), whereas expression of ectopic RRM2 was confirmed by expression of RRM2 mRNA measured by qRT-PCR using primers targeting the open reading frame (ORF) region and immunoblotting (Figures 5A and 5E). Indeed, compared with cells expressing shRRM2 alone, ectopic RRM2 expression rescued the aberrant DNA replication induced by shRRM2 (Figure 5B). Additionally, the DDR induced by shRRM2 was also suppressed by ectopic RRM2. Formation of γH2AX and 53BP1 foci (Figures 5C and 5D) and γH2AX and p53 expression (Figure 5E) were significantly lower in cells expressing both shRRM2 and ectopic RRM2 compared with shRRM2 alone. Furthermore, expression of markers of senescence such as SA-β-gal activity (Figures 5F and 5G) and upregulation of p21 (Figure 5H) was inhibited by ectopic RRM2 in the shRRM2-expressing cells. Moreover, ectopic RRM2 was sufficient to rescue the senescence-associated cell-cycle exit induced by RRM2 knockdown, as demonstrated by upregulation of cyclin A and pS10H3 (Figure 5H), increased BrdU incorporation

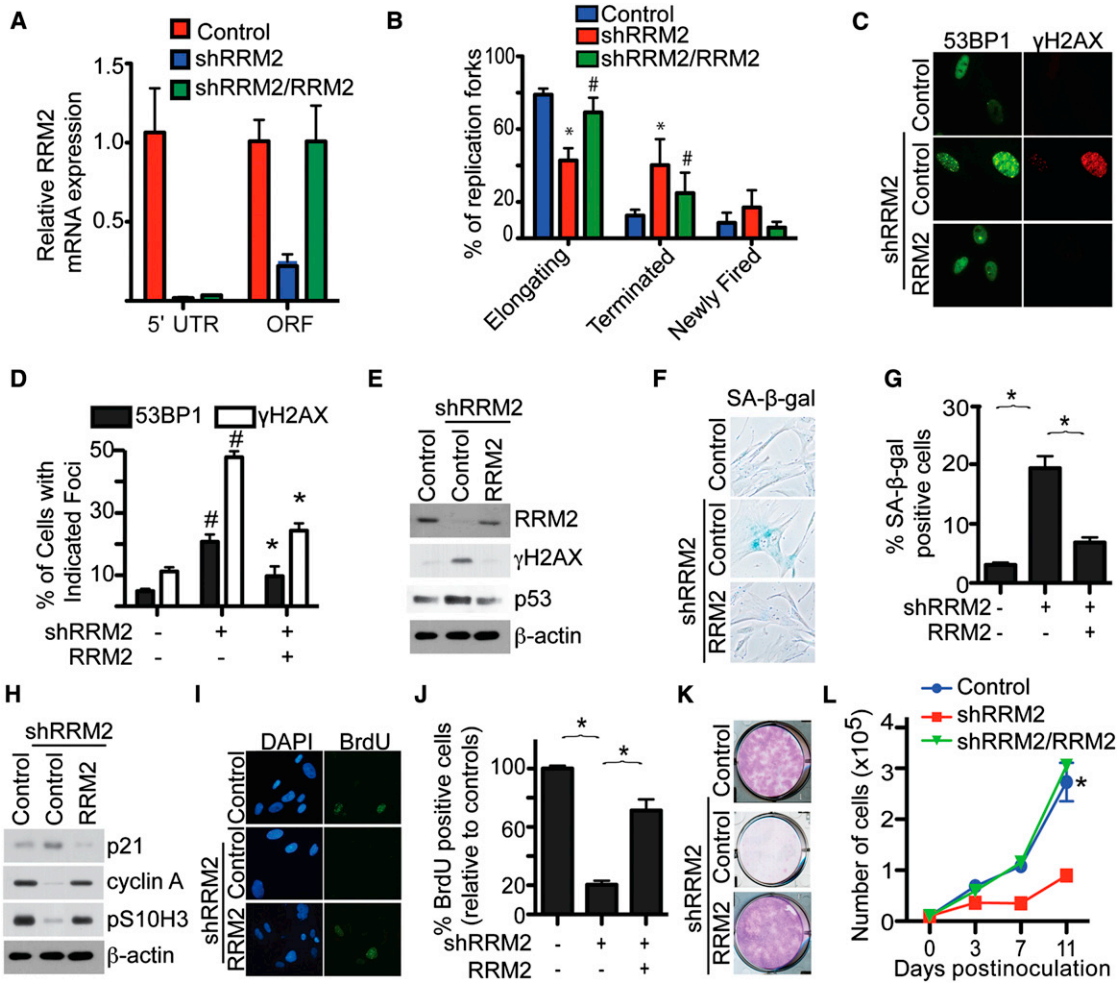

Figure 5. Knockdown of RRM2 Decreases dNTP Levels and Induces Senescence of Primary Human Fibroblasts

(A) IMR90 cells were infected with a lentivirus-encoding shRRM2 that targets the 5′ UTR of the human *RRM2* gene together with a retrovirus encoding a control or WT RRM2. On day 6, expression of RRM2 mRNA was determined by qRT-PCR using primers designed to its 5′ UTR (only amplifies endogenous but not ectopic RRM2 mRNA) or its ORF (amplifies both endogenous and ectopic RRM2 mRNA). Mean of three independent experiments with SEM is shown.

(B) Same as (A) but examined for DNA replication dynamics using the DNA-combing technique on day 2. Mean of three independent experiments with SEM is shown. *$p < 0.05$ control versus shRRM2; #$p < 0.05$ shRRM2 alone versus shRRM2/RRM2.

(C) Same as (A) but examined for formation of 53BP1 and γH2AX foci by immunofluorescence at day 6.

(D) Quantification of (C). Mean of three independent experiments with SEM is shown. #$p < 0.001$ versus vector controls; *$p < 0.001$ versus shRRM2-only cells.

(E) Same as (A) but examined for RRM2, γH2AX, p53, and β-actin expression by immunoblotting.

(F) Same as (A) but stained for SA-β-gal activity.

(G) Quantification of (F). Mean of three independent experiments with SEM is shown. *$p < 0.001$.

(H) Same as (A) but examined for p21, cyclin A, pS10H3, and β-actin by immunoblotting.

(I) Same as (A) but labeled with BrdU for 1 hr, and the incorporated BrdU was visualized by immunofluorescence. DAPI counterstaining was used to visualize nuclei.

(J) Quantification of (I). The relative percentage of BrdU-positive cells was calculated against vector controls. Mean of three independent experiments with SEM is shown. *$p < 0.001$.

(K) Same as (A), but an equal number of the indicated cells were seeded in 6-well plates. After 2 weeks, the plates were stained with 0.05% crystal violet in PBS to visualize colony formation. Shown are representative images from three independent experiments.

(L) Same as (K), but the number of cells was counted at the indicated time points. Mean of three independent experiments with SEM is shown. *$p < 0.001$ compared with cells expressing shRRM2 alone.

See also Figure S5.

(Figures 5I and 5J), colony formation (Figure 5K), and cell growth (Figure 5L) compared to shRRM2 alone. Notably, the ectopically expressed RRM2 levels were comparable to its endogenous level (Figures 5A and 5E), suggesting that the observed effects are not due to supraphysiological levels of RRM2 expression. Together, we conclude that knockdown of

RRM2 is sufficient to trigger aberrant DNA replication, the DDR, and senescence in primary human cells.

Ectopic RRM2 Expression Is Sufficient to Overcome the Stable OIS-Associated Cell Growth Arrest

We next sought to determine whether downregulation of RRM2 is necessary for the OIS-associated cell growth arrest. Toward this goal, we ectopically expressed RRM2 in RAS-infected cells. Compared with controls, ectopic RRM2 suppressed markers of senescence such as SA-β-gal activity and SAHF formation (Figures 6A and 6B) and upregulation of p16 and p21 (Figure 6C). Indeed, ectopic RRM2 suppressed the OIS-associated cell-cycle exit, as evidenced by the significant increase in cyclin A and pS10H3 expression (Figure 6C) and BrdU incorporation (Figures 6D and 6E). Ectopic RRM2 significantly suppressed the OIS-associated growth arrest as determined by colony-formation assays (Figure 6F) and cell growth curves (Figure 6G). Of note, to limit the effects of supraphysiological levels of RRM2 expression, we expressed the ectopic RRM2 at a level lower than that of control cells (Figure 6C). Importantly, the observed effects correlated with the rescue of dNTP levels by ectopic RRM2 in these cells (Figure 6H), further supporting the idea that RRM2 downregulation plays a major role in decreasing dNTP levels during OIS. In addition, ectopic RRM2 significantly suppressed the aberrant DNA replication observed during RAS-induced senescence (Figure 6I). This result suggests that RRM2 suppresses aberrant DNA replication by rescuing the decrease in dNTP levels. Likewise, the DDR was also suppressed by ectopic RRM2, as demonstrated by a decrease in the formation of 53BP1 and γH2AX foci (Figures 6J and 6K) as well as a decrease in p53 and γH2AX protein expression (Figure 6L). Based on these data, we conclude that RRM2 downregulation is necessary for senescence, and restoration of dNTP levels by ectopic RRM2 expression suppresses senescence.

We found that exogenous nucleosides are sufficient to overcome the OIS-associated cell growth arrest in established senescent cells (Figure 2). Because ectopic RRM2 is sufficient to rescue the decrease in dNTP levels during senescence (Figure 6H), we next sought to determine whether ectopic RRM2 expression is sufficient to overcome the stable OIS-associated cell growth arrest in established senescent cells. To do so, stably arrested senescent cells induced by RAS were infected with a lentivirus encoding RRM2 (which can infect growth-arrested, nondividing cells), and markers of senescence and cell cycle were examined. Compared with controls, markers of senescence such as SA-β-gal activity and p16 expression were suppressed by the lentivirus-mediated RRM2 expression (Figures 6M–6O). Significantly, expression of RRM2 was able to overcome the stable OIS-associated arrest, as evidenced by both increased pS10H3 expression and marked cell growth (Figures 6O and 6P). These observations were not due to a loss of RAS expression because RAS was expressed at similar levels in both control and RRM2-expressing cells (Figure 6O). Together, these data indicate that RRM2 repression is necessary for maintenance of the stable senescence-associated cell growth arrest in established senescent cells.

RRM2 Repression Correlates with Senescence Status in Human Nevi and Malignant Melanoma Harboring Oncogenic BRAF or NRAS

We next sought to determine the importance of our findings in a pathologically relevant model. Benign human nevi harboring activated oncogenes are comprised of oncogene-induced senescent melanocytes (Michaloglou et al., 2005). In addition, there is evidence to suggest that the progression of benign nevi with oncogenic BRAF or NRAS into malignant melanoma correlates with OIS bypass (Dankort et al., 2007; Dhomen et al., 2009; Kuilman et al., 2010). Thus, we sought to validate our findings by examining RRM2 expression in human benign nevi and malignant melanoma specimens. First, we determined whether RRM2 is downregulated during oncogenic BRAF or NRAS-induced senescence of primary human melanocytes. Indeed, RRM2 expression was significantly inhibited during senescence of melanocytes induced by oncogenic BRAF or NRAS (Figures 7A–7C and S6A–S6C). Similar to what we observed in primary human fibroblasts (Figure 1), exogenous nucleosides were able to suppress senescence induced by oncogenic BRAF in primary human melanocytes (Figures S6D–S6F). These results suggest that RRM2 expression may promote melanoma by suppressing oncogenic BRAF or NRAS-induced senescence.

We also determined that RRM2 expression was significantly increased in human melanoma cells harboring oncogenic BRAF or NRAS compared to normal human melanocytes (Figure 7D). Notably, it has previously been demonstrated that supraphysiological levels of RRM2 promote tumorigenesis by causing genomic instability and the DDR (D'Angiolella et al., 2012; Xu et al., 2008). Consistently, we observed that physiological levels of RRM2 suppress oncogenic RAS-induced DDR (Figure 6), whereas DDR markers such as γH2AX remain high in RAS-infected cells expressing supraphysiological levels of RRM2 (Figures S6G and S6H).

We next compared expression of RRM2, the senescence marker p16, and the cell proliferation marker Ki67 in a cohort of human benign nevi and melanoma specimens harboring oncogenic BRAF or NRAS (Table S1). Strikingly, RRM2 expression was nearly negative in human nevi with oncogenic BRAF or NRAS, whereas the expression of RRM2 was significantly higher in the melanoma specimens with oncogenic BRAF or NRAS (Figures 7E and 7F). Consistently, expression of p16 was significantly higher in benign human nevi compared to malignant melanomas (Figures 7E and S6I). In contrast, expression of Ki67 was negative in benign human nevi and significantly higher in melanoma specimens (Figures 7E and S6J). These results are consistent with the idea that the supraphysiological levels of RRM2 observed in melanoma specimens contribute to melanoma by suppressing oncogenic BRAF or NRAS-induced senescence. We next determined whether RRM2 expression negatively correlates with survival in patients with melanoma harboring oncogenic BRAF or NRAS. Indeed, high RRM2 expression significantly correlates with poor overall survival in these patients with melanoma (Figure 7G). In contrast, expression of RRM1 does not correlate with the survival of patients with melanoma harboring oncogenic BRAF or NRAS (Figure S6K). We conclude that RRM2 repression correlates with

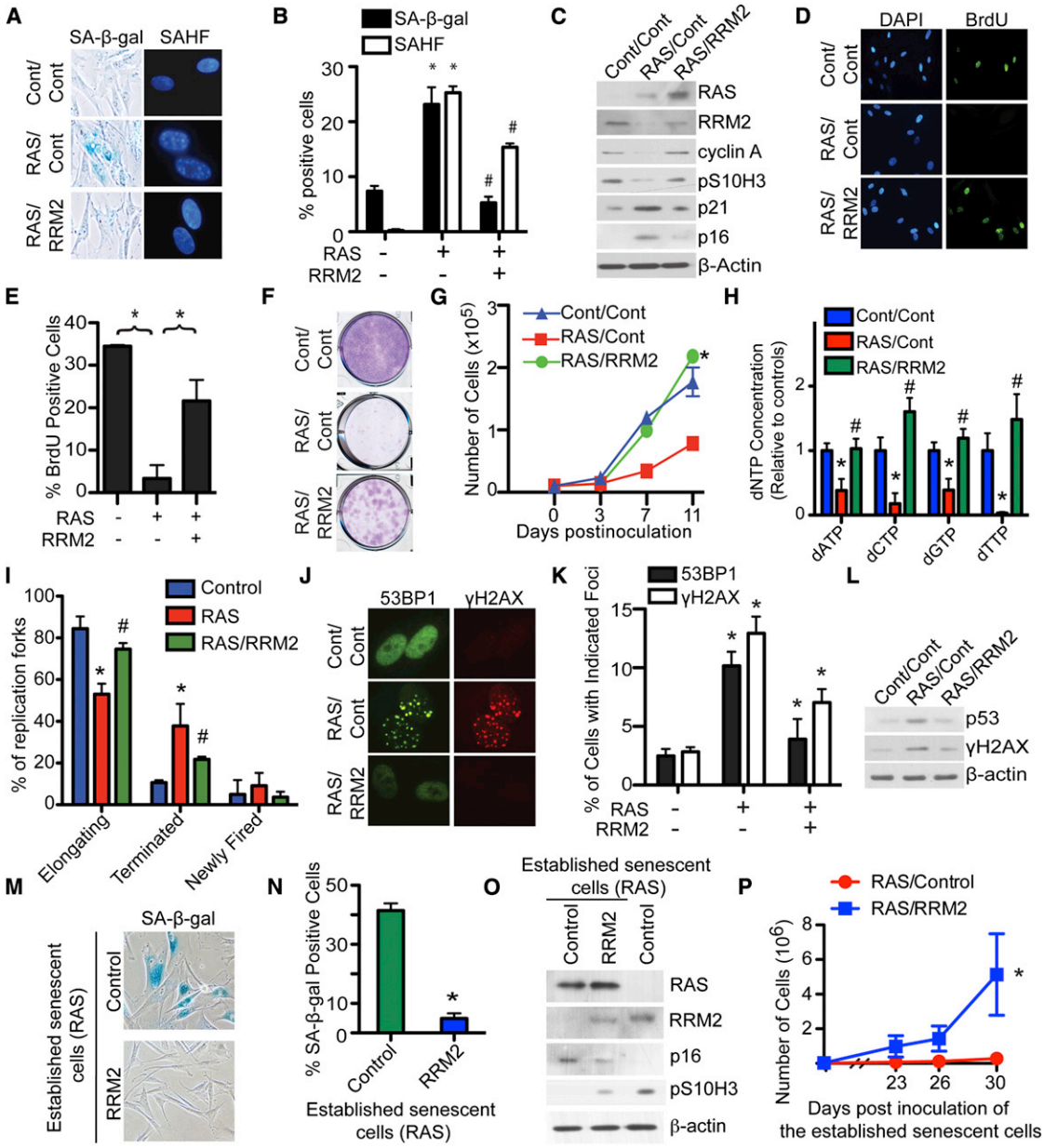

Figure 6. Ectopic RRM2 Expression Suppresses Senescence and Is Sufficient to Overcome the Stable OIS-Associated Cell Growth Arrest

(A) IMR90 cells were coinfected with retrovirus-encoding control or RAS together with or without RRM2. Cells were examined for SA-β-gal activity or SAHF expression on day 6.

(B) Quantification of (A). Mean of three independent experiments with SEM is shown. *$p < 0.05$ control versus RAS; #$p < 0.05$ RAS alone versus RAS/RRM2.

(C) Same as (A) but examined for RAS, RRM2, cyclin A, pS10H3, p21, p16, and β-actin expression by immunoblotting.

(D) Same as (A), but the cells were labeled with BrdU for 1 hr, and the BrdU incorporation was visualized by immunofluorescence. DAPI counterstaining was used to visualize nuclei.

(E) Quantification of (D). Mean of three independent experiments with SEM is shown. *$p < 0.01$.

(F) Same as (A), but an equal number of the indicated cells were seeded in 6-well plates. After 2 weeks, the plates were stained with 0.05% crystal violet in PBS to visualize colony formation. Shown are representative images from three independent experiments.

(G) Same as (F), but the number of cells was counted at the indicated time points. Mean of three independent experiments with SEM is shown. *$p < 0.01$.

(H) Same as (A), but on day 2, the concentrations of all four dNTPs were examined. $p < 0.05$ control versus RAS (*) and $p < 0.05$ RAS alone versus RAS/RRM2 (#). Mean of three independent experiments with SEM is shown.

(I) Same as (H) but examined for DNA replication dynamics using the DNA-combing technique on day 2. Mean of three independent experiments with SEM is shown. *$p < 0.05$ control versus RAS; #$p < 0.05$ RAS alone versus RAS/RRM2.

(J) Same as (A) but examined for the formation of 53BP1 and γH2AX foci by immunofluorescence at day 6.

(K) Quantification of (J). Mean of three independent experiments with SEM is shown. *$p < 0.05$.

(legend continued on next page)

the senescence status of human benign nevi and melanoma specimens, and high RRM2 expression significantly correlates with worse overall survival in patients with melanoma.

Finally, we wanted to determine whether melanoma cells harboring activated oncogenes can be driven to undergo senescence by knockdown of RRM2. To do this, UACC-62 human melanoma cells were infected with two individual shRRM2s. The knockdown efficacy of shRRM2s in UACC-62 cells was confirmed by immunoblotting (Figure 7H). The growth of UACC-62 cells was notably inhibited by knockdown of RRM2, as determined by cell growth curves (Figure 7I) and colony formation (Figure 7J). Interestingly, the DDR marker γH2AX was upregulated by RRM2 knockdown (Figure 7H). To determine whether these cells were undergoing senescence, SA-β-gal activity was assessed. Indeed, UACC-62 cells infected with shRRM2 had significantly increased SA-β-gal activity compared to controls (Figures 7K and 7L). Similar results were also obtained with another melanoma cell line, WM164 (Figures S6L–S6P), suggesting that the observed effects are not cell line specific. These results demonstrate that knockdown of RRM2 in melanoma cells suppresses the growth of these cells by triggering cellular senescence.

DISCUSSION

In this study, we demonstrate that a decrease in dNTP levels underlies the establishment and maintenance of the stable OIS-associated cell growth arrest. Mechanistically, we discovered that the decrease in dNTP levels is due to the transcriptional repression of the *RRM2* gene through recruitment of E2F7 prior to the senescence-associated cell-cycle exit. This correlates with aberrant DNA replication and coincides with the DDR during OIS. Notably, RRM2 downregulation is both necessary and sufficient for senescence, which correlates with its effects on the changes in cellular dNTP levels. Significantly, we demonstrated that suppression of nucleotide metabolism through RRM2 repression is necessary for maintenance of the stable OIS-associated cell growth arrest because established senescent cells can reenter the cell cycle after expression of ectopic RRM2. Underscoring the physiological relevance of the current discovery, we showed that RRM2 repression positively correlates with the senescence status of melanocytes in human benign nevi and melanoma specimens harboring oncogenic BRAF or NRAS. Additionally, high RRM2 expression correlates with poor overall survival in patients with melanoma harboring oncogenic BRAF or NRAS. Knockdown of RRM2 in human melanoma cells with activated oncogenes drives senescence of these cells, supporting the hypothesis that RRM2 promotes melanoma by suppressing the senescence tumor suppression mechanism.

We show that addition of exogenous nucleosides in established senescent cells is able to overcome the senescence-associated cell growth arrest (Figure 2). In addition, knockdown of RRM2 expression drives senescence and the associated cell growth arrest (Figures 5 and S5). Conversely, ectopic RRM2 is sufficient to overcome the stable senescence-associated cell growth arrest (Figure 6). These observed effects correlate with the changes in dNTP levels in these cells (Figures 5, 6, and S5). Significantly, RRM2 repression, which drives the decrease in dNTP levels, occurs prior to the senescence-associated cell-cycle exit (Figures 4A and 4B), demonstrating that the observed effects are not a consequence of senescence or its associated cell growth arrest. These results support the premise that the decrease in dNTP levels induced by RRM2 repression is necessary and sufficient for establishing and maintaining the stable senescence-associated cell growth arrest induced by activated oncogenes.

OIS is characterized by aberrant DNA replication during the S phase of the cell cycle, which triggers the DDR (Bartkova et al., 2006; Di Micco et al., 2006). Here, we show that dNTP levels are decreased prior to the OIS-associated cell-cycle exit (Figure 3A), and addition of exogenous nucleosides significantly rescues the aberrant DNA replication and DDR during OIS (Figures 1D, 1E, 3B, and 3C). These data indicate that there is a correlation between the decrease in dNTP pools and aberrant DNA replication and DDR during OIS. However, the effect of nucleosides on OIS is not a consequence of DDR because senescence induced by DNA-damaging agents such as doxorubicin and etoposide is not affected by exogenous nucleosides (Figures S1B–S1I). This further supports the premise that the decrease in dNTP levels is specifically linked to aberrant DNA replication during OIS. Indeed, RRM2 knockdown decreases dNTP levels and triggers aberrant DNA replication and the DDR (Figures 5B–5D and S5C–S5E). Conversely, ectopic RRM2 rescues the decrease in dNTP levels and suppresses the aberrant DNA replication and DDR induced by activated oncogenes (Figures 6H–6K). Together, these data support a model whereby oncogene-induced repression of RRM2 decreases the dNTP levels, which triggers aberrant DNA replication and the DDR and, ultimately, OIS-associated cell growth arrest. It is possible that the DDR triggered by aberrant DNA replication is irreparable in the context of oncogene activation because of the lack of dNTPs due to RRM2 repression. This causes persistent DDR observed in established senescent cells (Rodier et al., 2009) and underlies the stable OIS-associated cell growth arrest.

One of the classical examples of OIS as a tumor suppression mechanism is melanocytic nevi arising from oncogenic BRAF or NRAS (Kuilman et al., 2010). The stable growth arrest observed in these lesions is thought to prevent transformation of these cells into malignant melanoma (Mooi and Peeper, 2006). Here,

(L) Same as (A) but examined for p53, γH2AX, and β-actin expression by immunoblotting.
(M) IMR90 cells were infected with RAS-encoding retrovirus. On day 6, established senescent cells were infected with a lentivirus encoding RRM2 or an empty vector control. After an additional 14 days, the cells were stained for SA-β-gal activity.
(N) Quantification of (M). Mean of three independent experiments with SEM is shown. *$p < 0.001$.
(O) Same as (M) but examined for RAS, RRM2, p16, pS10H3, and β-actin expression by immunoblotting.
(P) Same as (M), but an equal number of cells were inoculated in 6-well plates, and the number of cells was counted at the indicated time points. Mean of three independent experiments with SEM is shown. *$p < 0.05$.

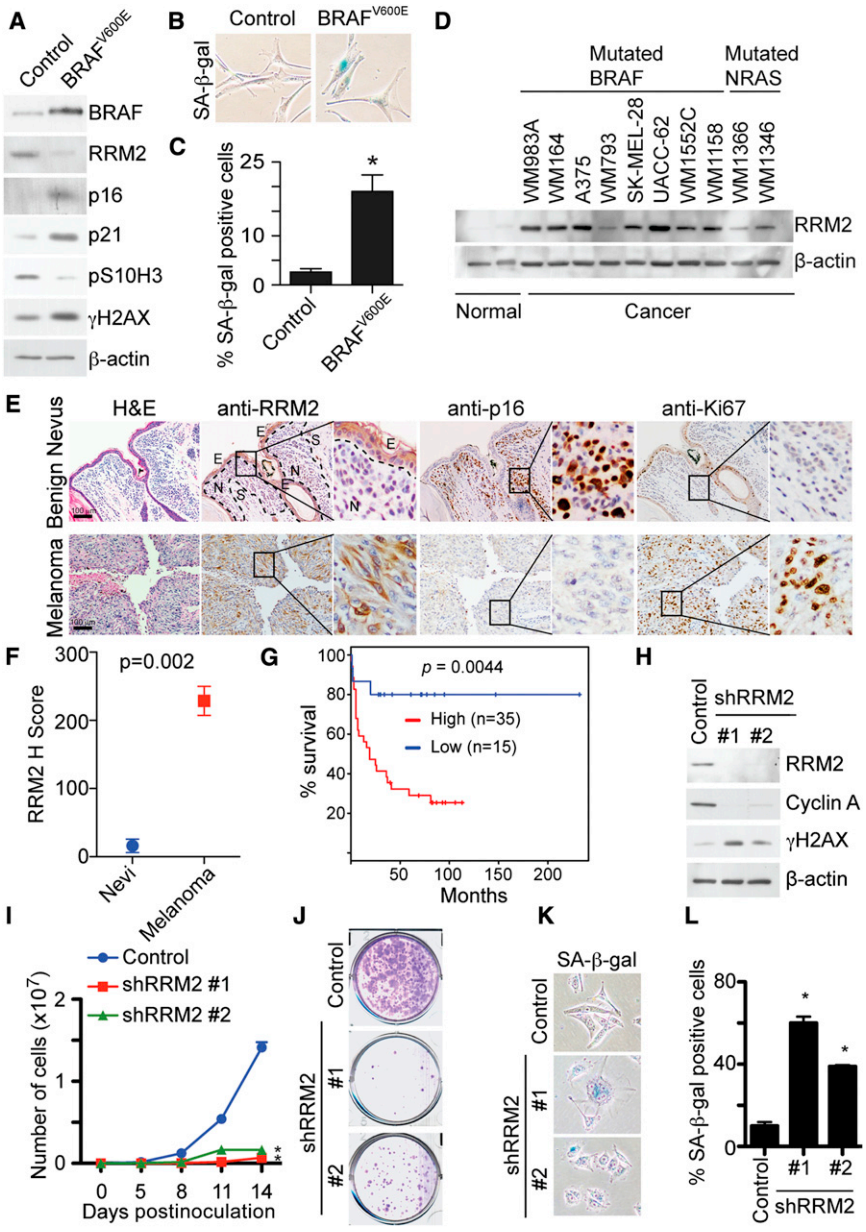

Figure 7. RRM2 Is Repressed in Human Benign Nevi, whereas Overexpressed in Melanoma; Knockdown of RRM2 Drives Senescence of Melanoma Cells

(A) Melanocytes were infected with a lentivirus encoding control or BRAF^{V600E}. At 21 days after infection, cells were examined for BRAF, RRM2, p16, p21, pS10H3, γH2AX, and β-actin expression by immunoblotting.

(B) Same as (A) but examined for SA-β-gal activity.

(C) Quantification of (B). Mean of two independent experiments with SEM is shown. *$p < 0.01$.

(D) RRM2 and β-actin expression in two individual isolations of normal human melanocytes and the indicated human melanoma cell lines by immunoblotting is shown. Mutation status of BRAF and NRAS of the selected cell lines is indicated.

(E) Immunohistochemical staining of RRM2, p16, and Ki67 in benign human nevus (N) and human melanoma tissue specimens harboring oncogenic BRAF or NRAS. Shown are examples of a benign human nevus and a human melanoma tissue harboring oncogenic BRAF^{V600E}. S, stroma; E, epidermal compartments.

(F) Quantification of RRM2 staining in (E). Expression of RRM2 in benign human nevi (n = 5) and melanoma tissue specimens (n = 7) was quantified using the histological score. Mean of three independent experiments with SEM is shown.

(G) A high level of RRM2 expression correlates with shorter overall survival in human patients with melanoma harboring oncogenic BRAF or NRAS. The univariate overall survival curve (Kaplan-Meier method) for patients with melanoma (n = 50) with high or low RRM2 expression is detailed in Experimental Procedures.

(H) UACC-62 human melanoma cells were infected with control or two individual shRRM2s encoding lentivirus. RRM2, cyclin A, γH2AX, and β-actin expression was determined by immunoblotting.

(I) Same as (H), but an equal number of cells were seeded in 6-well plates, and the number of cells was counted at the indicated time points. Mean of three independent experiments with SEM is shown. *$p < 0.05$ compared with controls.

(J) Same as (I), but after 2 additional weeks, the plates were stained with 0.05% crystal violet in PBS to visualize colony formation. Shown are representative images of three independent experiments.

(K) Same as (H) but stained for SA-β-gal activity.

(L) Quantification of (K). Mean of three independent experiments with SEM is shown. *$p < 0.05$ compared with controls.

See also Figure S6 and Table S1.

we found that RRM2 repression correlates with senescence status in human melanocytic nevi and melanoma specimens harboring oncogenic BRAF or NRAS (Figure 7). Interestingly, as previously reported by Michaloglou et al. (2005), expression of the senescence marker p16 in melanocytic nevi is heterogeneous with a proportion of negative expression cells (Figure 7E). In contrast, RRM2 repression occurs in nearly all melanocytes within the benign nevi (Figures 7E and 7F). This suggests that suppression of nucleotide metabolism plays a broader role in maintaining the OIS-associated stable cell growth arrest, such as the one observed in melanocytic nevi, compared to p16. Together, these findings are consistent with the idea that RRM2 repression is necessary for the stable cell growth arrest observed in OIS-associated benign lesions such as melanocytic nevi.

Cellular dNTP levels play a role in regulating cell proliferation by controlling DNA synthesis (Reichard, 1988). Here, we show that activation of oncogenes decreases dNTP levels in primary human cells prior to OIS-associated cell growth arrest due to oncogene-induced RRM2 downregulation (Figures 3 and 6H).

This suggests that RRM2 downregulation leads to an uncoordinated cell proliferation and dNTP supply, which ultimately leads to senescence and the associated cease of proliferation. Consistently, changes in nucleotide metabolism have been implicated in the early stages of cancer development. For example, the viral oncogenic protein HPV16 E6/7 induces genomic instability by suppressing dNTP synthesis (Bester et al., 2011). Furthermore, we show that RRM2 repression correlates with senescence status in human nevi or melanoma specimens harboring oncogenic BRAF or NRAS (Figures 7 and S6). Consistently, knockdown of RRM2 drives the senescence of melanoma cells harboring activated oncogenes (Figures 7H–7L and S6L–S6P). These data are consistent with a model whereby RRM2 expression regulates the OIS-associated cell growth arrest by acting as a key switch for the coordinated cell proliferation and dNTP supply.

We show that RRM2 is downregulated at the transcriptional level during OIS (Figures 4C and 4D). In addition, we show that RRM2 transcriptional repression correlates with an enhanced association with E2F7, a transcriptional repressor, with the promoter of the *RRM2* gene (Figure 4E). This correlates with a simultaneous decrease in binding of transcriptional activator E2F1 to the *RRM2* gene promoter. Indeed, E2F7 upregulation demonstrated the same kinetics as RRM2 downregulation during OIS (Figure 4F). Consistent with our observation, E2F7 has recently been shown to be upregulated during the early stages of senescence (Aksoy et al., 2012). In addition, RRM2 has also been shown to be regulated by c-Myc (Liu et al., 2008), a key regulator of the nucleotide biosynthetic pathway (Dang, 1999, 2011). Thus, it is plausible that c-Myc may cooperate indirectly with E2F7 and E2F1 in regulating RRM2 transcription prior to the senescence-associated cell-cycle exit.

We found that RRM2 is significantly overexpressed in melanoma cells (Figures 7D–7F). Notably, supraphysiological levels of RRM2 can lead to genomic instability, DNA damage, and tumorigenesis by causing an imbalance in dNTP pools (D'Angiolella et al., 2012; Xu et al., 2008). Here, we show that supraphysiological levels of RRM2 observed in melanoma cells correlate with loss of expression of markers of senescence in melanoma specimens (Figure 7). In addition, we found that markers of the DDR remain high in RAS-infected primary human fibroblasts expressing supraphysiological levels of RRM2 (Figures S6G and S6H). These data support the notion that supraphysiological levels of RRM2 suppress OIS and simultaneously promote genomic instability by allowing error-prone replication due to an imbalance in dNTP pools, which ultimately drives tumorigenesis. These data also demonstrate the important role of RRM2 in cancer development by controlling dNTP pools. Indeed, RRM2 knockdown in human melanoma cells harboring oncogenic BRAF suppressed the proliferation of these cells by triggering senescence (Figures 7H–7L and S6L–S6P). The p53 and pRB tumor suppressor pathways are key senescence effectors (Campisi and d'Adda di Fagagna, 2007; Courtois-Cox et al., 2008; Kuilman et al., 2010). Notably, p53 is mutated in the WM164 cell line (Weiss et al., 1993). In addition, p16 is deleted in the UACC-62 cell line (Ikediobi et al., 2006) and mutated in the WM164 cell line (Ohta et al., 1994). However, knockdown of RRM2 in these cells was able to induce senescence (Figures 7H–7L and S6L–S6P). Therefore, senescence induced by RRM2 inhibition in melanoma cells is independent of both p53 and p16. This indicates that human cancer cells that lack functional p53 and p16 retain the capacity to undergo senescence through suppressing RRM2. These data suggest that inhibition of the nucleotide biosynthetic pathway by suppressing RRM2 represents a bona fide target for driving cancer cells to undergo senescence.

In summary, suppression of nucleotide metabolism via RRM2 repression underlies the establishment and maintenance of the stable cell growth arrest, the hallmark that characterizes OIS as an important tumor suppression mechanism. These data place altered nucleotide metabolism at the heart of OIS regulation and provide the molecular basis by which the stable OIS-associated cell growth arrest is established and maintained.

EXPERIMENTAL PROCEDURES

Retrovirus and Lentivirus Infections

Retrovirus production and transduction were performed as described previously (Tu et al., 2011; Ye et al., 2007; Zhang et al., 2005) using Phoenix cells to package the infection viruses (Dr. Gary Nolan, Stanford University). Lentivirus was packaged using the ViraPower Kit (Invitrogen, Carlsbad, CA, USA) following the manufacturer's instructions and as described previously (Li et al., 2010; Tu et al., 2011; Ye et al., 2007). Cells infected with viruses encoding the puromycin-resistance gene were selected in 3 μg/ml puromycin.

FACS for C_{12}FDG Expression

Cells were incubated with 33 μM C_{12}FDG (Invitrogen) for 1 hr as described previously by Debacq-Chainiaux et al. (2009). After rinsing with PBS, C_{12}FDG-positive cells were sorted using a FACS ARIAII (BD Biosciences, San Jose, CA, USA).

DNA-Combing Analysis

Cells were pulse labeled for 10 min with medium containing 2 mM of BrdU (Sigma-Aldrich), washed twice with PBS, incubated in regular medium for 20 min, and then chased for 20 min with medium containing 2 mM iododeoxyuridine (IdU; Sigma-Aldrich). Harvesting and spreading of DNA fibers were performed as previously described by Merrick et al. (2004). The DNA fibers were stained with antibodies to BrdU (Abcam) and IdU (Fitzgerald Industries, Acton, MA, USA), and the staining was visualized using secondary antibodies labeled with FITC and Cy3, respectively. DNA fibers were counterstained with a primary antibody to ssDNA (Millipore) and were visualized with a secondary antibody labeled with Alexa Fluor 350 (Invitrogen), allowing the exclusion of any broken or tangled fibers. DNA replication forks were scored as elongating, terminated, or newly fired, as previously described by Bartkova et al. (2006).

Measurement of dNTP Concentrations in Cells

Briefly, 5×10^6 cells were harvested and resuspended in 80% methanol. Cells were vortexed and stored at −20°C overnight. Next, cells were boiled for 3 min and centrifuged at 4°C at 17,000 × *g* for 20 min. Supernatants were harvested and dried using a vacuum centrifuge. Pellets were resuspended in nuclease-free water and stored at −20°C until use. dNTP concentration was measured as previously described by Wilson et al. (2011).

ChIP Analysis

ChIP in control and RAS-infected IMR90 cells was performed at day 2 as previously described (Zhang et al., 2007b) using antibodies against E2F1 (Santa Cruz Biotechnology), E2F7 (Santa Cruz Biotechnology), or an isotype-matched IgG control. Immunoprecipitated DNA was analyzed using SYBR Green qPCR Mastermix (SA Biosciences, Valencia, CA, USA) against the human *RRM2* gene promoter region containing the E2F1/E2F7 binding site using the following primers: forward, 5′-CTCCAGCTCCTGGCCTCAA-3′, and reverse, 5′-RCCGCGTGGACTGTTAATGC-3′.

Immunofluorescence, BrdU Labeling, and SA-β-Gal Staining

Immunofluorescence staining and BrdU labeling were performed as described previously using antibodies described above (Tu et al., 2011; Zhang et al., 2005, 2007a, 2007b). SA-β-gal staining was performed as previously described (Dimri et al., 1995). For quantification, a minimum of 200 cells from each group was examined.

Please see the Extended Experimental Procedures for further details.

SUPPLEMENTAL INFORMATION

Supplemental Information includes six figures, one table, and Extended Experimental Procedures and can be found with this article online at http://dx.doi.org/10.1016/j.celrep.2013.03.004.

LICENSING INFORMATION

ACKNOWLEDGMENTS

We thank Drs. Dario Altieri, Maureen Murphy, and Ronen Marmorstein for comments. We would also like to thank Dr. Greg Enders for the p16 antibody. We thank Jeffery Faust, David Ambrose, and Scott Weiss in the Wistar Institute Flow Cytometry facility for technical help. R.Z. is an Ovarian Cancer Research Fund Liz Tilberis Scholar. This work was supported by a NIH/NCI grant (R01CA160331 to R.Z.), a DoD Ovarian Cancer Academy Award (OC093420 to R.Z.), by the FWF-Austrian Science Fund (L590-B12 to S.N.W.), and an NIH/NCI training grant (T32CA9171-35 to K.M.A.). Support of core facilities used in this study was provided by Cancer Center Support Grant CA010815 to The Wistar Institute.

Received: October 31, 2012
Revised: January 28, 2013
Accepted: March 1, 2013
Published: April 4, 2013

REFERENCES

Aksoy, O., Chicas, A., Zeng, T., Zhao, Z., McCurrach, M., Wang, X., and Lowe, S.W. (2012). The atypical E2F family member E2F7 couples the p53 and RB pathways during cellular senescence. Genes Dev. *26*, 1546–1557.

Bartkova, J., Rezaei, N., Liontos, M., Karakaidos, P., Kletsas, D., Issaeva, N., Vassiliou, L.V., Kolettas, E., Niforou, K., Zoumpourlis, V.C., et al. (2006). Oncogene-induced senescence is part of the tumorigenesis barrier imposed by DNA damage checkpoints. Nature *444*, 633–637.

Bester, A.C., Roniger, M., Oren, Y.S., Im, M.M., Sarni, D., Chaoat, M., Bensimon, A., Zamir, G., Shewach, D.S., and Kerem, B. (2011). Nucleotide deficiency promotes genomic instability in early stages of cancer development. Cell *145*, 435–446.

Campisi, J. (2005). Senescent cells, tumor suppression, and organismal aging: good citizens, bad neighbors. Cell *120*, 513–522.

Campisi, J., and d'Adda di Fagagna, F. (2007). Cellular senescence: when bad things happen to good cells. Nat. Rev. Mol. Cell Biol. *8*, 729–740.

Chen, H.Z., Tsai, S.Y., and Leone, G. (2009). Emerging roles of E2Fs in cancer: an exit from cell cycle control. Nat. Rev. Cancer *9*, 785–797.

Courtois-Cox, S., Jones, S.L., and Cichowski, K. (2008). Many roads lead to oncogene-induced senescence. Oncogene *27*, 2801–2809.

Dang, C.V. (1999). c-Myc target genes involved in cell growth, apoptosis, and metabolism. Mol. Cell. Biol. *19*, 1–11.

Dang, C.V. (2011). Therapeutic targeting of Myc-reprogrammed cancer cell metabolism. Cold Spring Harb. Symp. Quant. Biol. *76*, 369–374.

D'Angiolella, V., Donato, V., Forrester, F.M., Jeong, Y.T., Pellacani, C., Kudo, Y., Saraf, A., Florens, L., Washburn, M.P., and Pagano, M. (2012). Cyclin F-mediated degradation of ribonucleotide reductase M2 controls genome integrity and DNA repair. Cell *149*, 1023–1034.

Dankort, D., Filenova, E., Collado, M., Serrano, M., Jones, K., and McMahon, M. (2007). A new mouse model to explore the initiation, progression, and therapy of BRAFV600E-induced lung tumors. Genes Dev. *21*, 379–384.

Debacq-Chainiaux, F., Erusalimsky, J.D., Campisi, J., and Toussaint, O. (2009). Protocols to detect senescence-associated beta-galactosidase (SA-betagal) activity, a biomarker of senescent cells in culture and in vivo. Nat. Protoc. *4*, 1798–1806.

Dhomen, N., Reis-Filho, J.S., da Rocha Dias, S., Hayward, R., Savage, K., Delmas, V., Larue, L., Pritchard, C., and Marais, R. (2009). Oncogenic Braf induces melanocyte senescence and melanoma in mice. Cancer Cell *15*, 294–303.

Di Micco, R., Fumagalli, M., Cicalese, A., Piccinin, S., Gasparini, P., Luise, C., Schurra, C., Garre', M., Nuciforo, P.G., Bensimon, A., et al. (2006). Oncogene-induced senescence is a DNA damage response triggered by DNA hyper-replication. Nature *444*, 638–642.

Dimri, G.P., Lee, X., Basile, G., Acosta, M., Scott, G., Roskelley, C., Medrano, E.E., Linskens, M., Rubelj, I., Pereira-Smith, O., et al. (1995). A biomarker that identifies senescent human cells in culture and in aging skin in vivo. Proc. Natl. Acad. Sci. USA *92*, 9363–9367.

Engström, Y., Eriksson, S., Jildevik, I., Skog, S., Thelander, L., and Tribukait, B. (1985). Cell cycle-dependent expression of mammalian ribonucleotide reductase. Differential regulation of the two subunits. J. Biol. Chem. *260*, 9114–9116.

Håkansson, P., Hofer, A., and Thelander, L. (2006). Regulation of mammalian ribonucleotide reduction and dNTP pools after DNA damage and in resting cells. J. Biol. Chem. *281*, 7834–7841.

Ikediobi, O.N., Davies, H., Bignell, G., Edkins, S., Stevens, C., O'Meara, S., Santarius, T., Avis, T., Barthorpe, S., Brackenbury, L., et al. (2006). Mutation analysis of 24 known cancer genes in the NCI-60 cell line set. Mol. Cancer Ther. *5*, 2606–2612.

Kuilman, T., Michaloglou, C., Mooi, W.J., and Peeper, D.S. (2010). The essence of senescence. Genes Dev. *24*, 2463–2479.

Li, H., Cai, Q., Godwin, A.K., and Zhang, R. (2010). Enhancer of zeste homolog 2 promotes the proliferation and invasion of epithelial ovarian cancer cells. Mol. Cancer Res. *8*, 1610–1618.

Liu, Y.C., Li, F., Handler, J., Huang, C.R., Xiang, Y., Neretti, N., Sedivy, J.M., Zeller, K.I., and Dang, C.V. (2008). Global regulation of nucleotide biosynthetic genes by c-Myc. PLoS One *3*, e2722.

Merrick, C.J., Jackson, D., and Diffley, J.F. (2004). Visualization of altered replication dynamics after DNA damage in human cells. J. Biol. Chem. *279*, 20067–20075.

Michaloglou, C., Vredeveld, L.C., Soengas, M.S., Denoyelle, C., Kuilman, T., van der Horst, C.M., Majoor, D.M., Shay, J.W., Mooi, W.J., and Peeper, D.S. (2005). BRAFE600-associated senescence-like cell cycle arrest of human naevi. Nature *436*, 720–724.

Mooi, W.J., and Peeper, D.S. (2006). Oncogene-induced cell senescence—halting on the road to cancer. N. Engl. J. Med. *355*, 1037–1046.

Narita, M., Nũnez, S., Heard, E., Narita, M., Lin, A.W., Hearn, S.A., Spector, D.L., Hannon, G.J., and Lowe, S.W. (2003). Rb-mediated heterochromatin formation and silencing of E2F target genes during cellular senescence. Cell *113*, 703–716.

Nordlund, P., and Reichard, P. (2006). Ribonucleotide reductases. Annu. Rev. Biochem. *75*, 681–706.

Ohta, M., Nagai, H., Shimizu, M., Rasio, D., Berd, D., Mastrangelo, M., Singh, A.D., Shields, J.A., Shields, C.L., Croce, C.M., et al. (1994). Rarity of somatic and germline mutations of the cyclin-dependent kinase 4 inhibitor gene, CDK4I, in melanoma. Cancer Res. *54*, 5269–5272.

Reichard, P. (1988). Interactions between deoxyribonucleotide and DNA synthesis. Annu. Rev. Biochem. *57*, 349–374.

Rodier, F., Coppé, J.P., Patil, C.K., Hoeijmakers, W.A., Muñoz, D.P., Raza, S.R., Freund, A., Campeau, E., Davalos, A.R., and Campisi, J. (2009).

Persistent DNA damage signalling triggers senescence-associated inflammatory cytokine secretion. Nat. Cell Biol. *11*, 973–979.

Serrano, M., Lin, A.W., McCurrach, M.E., Beach, D., and Lowe, S.W. (1997). Oncogenic ras provokes premature cell senescence associated with accumulation of p53 and p16INK4a. Cell *88*, 593–602.

Tu, Z., Aird, K.M., Bitler, B.G., Nicodemus, J.P., Beeharry, N., Zia, B., Yen, T.J., and Zhang, R. (2011). Oncogenic Ras regulates BRIP1 expression to induce dissociation of BRCA1 from chromatin, inhibit DNA repair, and promote senescence. Dev. Cell *21*, 1077–1091.

Weiss, J., Schwechheimer, K., Cavenee, W.K., Herlyn, M., and Arden, K.C. (1993). Mutation and expression of the p53 gene in malignant melanoma cell lines. Int. J. Cancer *54*, 693–699.

Wilson, P.M., Labonte, M.J., Russell, J., Louie, S., Ghobrial, A.A., and Ladner, R.D. (2011). A novel fluorescence-based assay for the rapid detection and quantification of cellular deoxyribonucleoside triphosphates. Nucleic Acids Res. *39*, e112.

Xu, X., Page, J.L., Surtees, J.A., Liu, H., Lagedrost, S., Lu, Y., Bronson, R., Alani, E., Nikitin, A.Y., and Weiss, R.S. (2008). Broad overexpression of ribonucleotide reductase genes in mice specifically induces lung neoplasms. Cancer Res. *68*, 2652–2660.

Yaswen, P., and Campisi, J. (2007). Oncogene-induced senescence pathways weave an intricate tapestry. Cell *128*, 233–234.

Ye, X., Zerlanko, B., Kennedy, A., Banumathy, G., Zhang, R., and Adams, P.D. (2007). Downregulation of Wnt signaling is a trigger for formation of facultative heterochromatin and onset of cell senescence in primary human cells. Mol. Cell *27*, 183–196.

Zhang, R., Poustovoitov, M.V., Ye, X., Santos, H.A., Chen, W., Daganzo, S.M., Erzberger, J.P., Serebriiskii, I.G., Canutescu, A.A., Dunbrack, R.L., et al. (2005). Formation of MacroH2A-containing senescence-associated heterochromatin foci and senescence driven by ASF1a and HIRA. Dev. Cell *8*, 19–30.

Zhang, R., Chen, W., and Adams, P.D. (2007a). Molecular dissection of formation of senescence-associated heterochromatin foci. Mol. Cell. Biol. *27*, 2343–2358.

Zhang, R., Liu, S.T., Chen, W., Bonner, M., Pehrson, J., Yen, T.J., and Adams, P.D. (2007b). HP1 proteins are essential for a dynamic nuclear response that rescues the function of perturbed heterochromatin in primary human cells. Mol. Cell. Biol. *27*, 949–962.